



Analysis on spectral gain characteristics of PPMgLN based quasi-phase-matching optical parametric amplification*

Hai-bin XU[†], Bo WU, Shuang-shuang CAI, Yong-hang SHEN

(State Key Laboratory of Modern Optical Instrumentation, Zhejiang University, Hangzhou 310027, China)

[†]E-mail: xhb.zd@163.com

Received Mar. 17, 2008; Revision accepted July 4, 2008; Crosschecked Feb. 9, 2009

Abstract: A deep understanding of the spectral gain characteristics of optical parametric oscillators (OPOs) and optical parametric amplifiers (OPAs) is important for a highly efficient optical parametric conversion. We numerically calculated the spectral gain characteristics of a quasi-phase-matching (QPM) parametric conversion process using the periodically poled 6% (mol/mol) MgO doped LiNbO₃ (PPMgLN) as the nonlinear crystal. In the simulation we utilized the approach of a transformative matrix of the periodically poled nonlinear medium, which results from the small-signal approximation of three-wave mixed nonlinear equations. Numerical simulation results show that: (1) The full width at half maximum (FWHM) of the spectral gain of the parametric process becomes wider with the increase of parametric wavelength and reaches the maximum at degeneration; (2) The gain coefficient decreases gradually with the increase of parametric wavelength; (3) The spectral gain bandwidth decreases correspondingly with the increase of the nonlinear material length; (4) There exists an optimal parametric wavelength band, which is most suitable for the high gain parametric conversion when pumped by a laser source with a wide wavelength band, such as the high power fiber laser.

Key words: Spectral gain full width at half maximum (FWHM), Quasi-phase matching (QPM), Optical parametric conversion, PPMgLN

doi:10.1631/jzus.A0820192

Document code: A

CLC number: O437.4; TN201

INTRODUCTION

Ever since the first presentation of optical parametric oscillators (OPOs) (Armstrong *et al.*, 1962), such a nonlinear optical conversion technique has found wide applications in many different fields due to its ability to produce strong and widely tunable laser. Especially, the quasi-phase-matching (QPM) OPO can realize a highly efficient optical frequency conversion by utilizing the periodically poled nonlinear materials (Jiang and Hasama, 2003; Zhu *et al.*, 2003; Feng *et al.*, 2007; Wu *et al.*, 2007; Xie and Fejer, 2007), and has the virtues of wide tunable laser output, low threshold, all-solidness, compactness, and

credible stability. In the past decade, with the development of fabrication technology on the periodically poled materials, the QPM-based OPO has been turning into one of the mainstreams of the tunable lasers and playing an increasingly important role in the fields of environment test, remote sensing, medical diagnosis and treatment, laser spectroscopy research, material processing, spatial data communications, photoelectric measurement, laser radar, and infrared count measurement (Chen *et al.*, 2001; Kulp *et al.*, 2002; Popp *et al.*, 2002; Stothard *et al.*, 2004). As one of the major periodically domain-reversed materials, the periodically poled lithium niobate (PPLN), in particular the magnesium oxide doped lithium niobate (PPMgLN), has found wide applications in a variety of optical frequency conversion systems. Due to the greatly improved resistance to photorefractive damage (Bryan *et al.*, 1984) of MgO-doped LiNbO₃ and

* Project supported by the National Natural Science Foundation of China (No. 60778001), and the National Basic Research Program (973) of China (No. 2007CB307003)

its much smaller coercive electric field intensity (Kuroda *et al.*, 1996; Huang *et al.*, 2001), the fabrication of larger volume size (Ishizuki *et al.*, 2003a; 2003b) PPMgLN becomes possible. And these advantages together make PPMgLN more suitable for optical frequency conversion applications with high power intensity.

In the parametric conversion process of an optical parametric amplifier (OPA) and an OPO, the parametric spectral gain bandwidth and gain coefficient in the nonlinear crystal greatly influence the conversion efficiency and the optical characteristics of the output parametric waves. Therefore, accurate information of the parametric gain coefficient, spectral bandwidth and some other factors under specific working conditions will be of great significance to the understanding and command of the corresponding frequency conversion process. It will clearly be important to optimize the structure parameters of the PPMgLN crystal, and then the whole parametric conversion process including the laser output.

By applying the small-signal approximation of three-wave coupling equations to a homogeneous nonlinear crystal and the matrix iterative methods of calculation, the spectral gain characteristics of an OPA are numerically simulated in this work. The OPA works at room temperature and uses the 6% (mol/mol) MgO doped PPMgLN as the nonlinear crystal. When compared with the experimental results obtained in a PPMgLN based OPO developed by our research group, some points have been confirmed. And this helps to convince that the results obtained can be helpful to designing practical applicable highly efficient OPOs and OPAs. The relevant calculation methods used in this study can be further implemented for the simulation of composite structural PPMgLN based OPAs and OPOs for higher conversion efficiency under high-power pumping.

THEORETICAL ANALYSIS

To derive the mathematical expression for the second-order nonlinear optical interactions in nonlinear media having periodic structures, general formulae should be introduced at first, which have been studied comprehensively in (McMullen, 1975). Consider three optical plane waves at frequencies ω_1 , ω_2 and ω_3 ($\omega_3=\omega_1+\omega_2$) with a form of

$$E_j(\omega_j, z, t) = E_j(z) \exp[i(k_j z - \omega_j t)], \quad j = 1, 2, 3, \quad (1)$$

where $E_j(z)$ is a complex factor including the slowly varying amplitude and phase due to nonlinear interaction, and k_j and ω_j are the wave vector and frequency of interaction waves respectively. When the waves propagate collinearly in a nonlinear medium, each wave is coupled with the other waves through nonlinear polarization. According to the approximations of (Milton, 1992), the Maxwell equations for electric fields at the three frequencies can be reduced to the following coupled-wave equations:

$$\frac{\partial}{\partial z} E_1(z) = i \frac{(2\pi)^2}{n_1 \lambda_1} \mu \chi^{\text{NL}} E_3(z) E_2^*(z) \exp(i\Delta k z), \quad (2a)$$

$$\frac{\partial}{\partial z} E_2(z) = i \frac{(2\pi)^2}{n_2 \lambda_2} \mu \chi^{\text{NL}} E_3(z) E_1^*(z) \exp(i\Delta k z), \quad (2b)$$

$$\frac{\partial}{\partial z} E_3(z) = i \frac{(2\pi)^2}{n_3 \lambda_3} \mu \chi^{\text{NL}} E_1(z) E_2(z) \exp(-i\Delta k z), \quad (2c)$$

where the nonlinear susceptibility χ^{NL} couples with the electric fields at each frequency; μ is the magnetic permeability in vacuum; n_j ($j=1, 2, 3$) is the (linear) refractive index at ω_j ($j=1, 2, 3$); λ_j ($j=1, 2, 3$) is the wavelength of each frequency in vacuum; Δk is defined as $\Delta k = k_3 - k_2 - k_1$.

In periodically poled materials, the effective nonlinear susceptibility of the n th domain can be written as follows:

$$\chi^{\text{NL}}(n) = (-1)^n \chi^{\text{NL}}. \quad (3)$$

Under the small-signal approximation, the intense pump beam at ω_3 is assumed to be non-depleted so that $E_3(z)$ is constant over the interaction length, and the parametric growth of the waves at ω_1 and ω_2 can then be described by the following two uncoupled equations:

$$\frac{\partial^2}{\partial z^2} E_j(z) - i\Delta k \frac{\partial}{\partial z} E_j(z) - G^2 E_j(z) = 0, \quad j = 1, 2, \quad (4a)$$

where

$$\xi_j = \frac{(2\pi)^2}{n_j \lambda_j} \mu \chi^{\text{NL}} E_3, \quad j = 1, 2, \quad (4b)$$

$$G^2 = \xi_1 \xi_2, \quad (4c)$$

$$G' = \sqrt{G^2 - (\Delta k / 2)^2}. \quad (4d)$$

The solutions for $E_j(z)$ are related to the input electric fields at z_0 according to

$$E_1(z) = \left\{ \cosh[G'(z - z_0)] - \frac{i\Delta k}{2G'} \sinh[G'(z - z_0)] \right\} \cdot \exp\left[\frac{1}{2}i\Delta k(z - z_0)\right] E_1(z_0) + i\frac{\xi_1}{G'} \sinh[G'(z - z_0)] \cdot \exp\left[\frac{1}{2}i\Delta k(z + z_0)\right] E_2^*(z_0), \quad (5a)$$

$$E_2^*(z) = \left\{ i\frac{\xi_2}{G'} \sinh[G'(z - z_0)] \exp\left[\frac{1}{2}i\Delta k(z + z_0)\right] \right\}^* E_1(z_0) + \left\{ \left\{ \cosh[G'(z - z_0)] - \frac{i\Delta k}{2G'} \sinh[G'(z - z_0)] \right\} \cdot \exp\left[\frac{1}{2}i\Delta k(z - z_0)\right] \right\}^* E_2^*(z_0). \quad (5b)$$

For periodically poled materials (Fig.1), all the domain length is assumed to be the same as L_c . Eqs.(5a) and (5b) are satisfied in each domain.

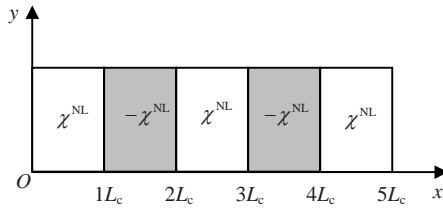


Fig.1 Structure diagram of the periodically poled nonlinear crystal

Therefore, the nonlinear transformative matrix in the n th domain can be written as follows:

$$\mathbf{M}(n) = \begin{pmatrix} m_{11}(n) & m_{12}(n) \\ m_{21}(n) & m_{22}(n) \end{pmatrix}, \quad (6)$$

where

$$m_{11}(n) = \left[\cosh(G'L_c) - \frac{i\Delta k}{2G'} \sinh(G'L_c) \right] \exp\left(\frac{1}{2}i\Delta kL_c\right),$$

$$m_{12}(n) = i\frac{(-1)^n \xi_1}{G'} \sinh(G'L_c) \exp\left[\frac{1}{2}i\Delta k(2n-1)L_c\right],$$

$$m_{21}(n) = \left\{ i\frac{(-1)^n \xi_2}{G'} \sinh(G'L_c) \exp\left[\frac{1}{2}i\Delta k(2n-1)L_c\right] \right\}^*,$$

$$m_{22}(n) = \left\{ \left[\cosh(G'L_c) - \frac{i\Delta k}{2G'} \sinh(G'L_c) \right] \exp\left(\frac{1}{2}i\Delta kL_c\right) \right\}^*.$$

Denoting the input electric fields just before the n th domain by $E_1(n-1)$ and $E_2(n-1)$, and the output electric fields following the n th domain by $E_1(n)$ and $E_2(n)$, the electric field conversion through the n th domain can be written as follows:

$$\begin{pmatrix} E_1(n) \\ E_2^*(n) \end{pmatrix} = \mathbf{M}(n) \begin{pmatrix} E_1(n-1) \\ E_2^*(n-1) \end{pmatrix}. \quad (7)$$

Given the input electric fields, the output parametric fields after N periodically poled domains can be calculated by repeatedly using Eq.(7).

NUMERICAL SIMULATION

The initial parameters and conditions used in the simulation are listed in Table 1, which made the simulation more close to the real situation. The PPMgLN [with 6% (mol/mol) doped MgO] was chosen as the domain-reversed nonlinear material.

Table 1 Initial parameters of the three-wave nonlinear conversion process

Wave	Wavelength (nm)	Intensity (V/pm)	Temperature (K)
Pump	1064	10^{-7}	300
Signal	1064	10^{-12}	300
Idle	1064	10^{-12}	300

The calculated parametric spectral gain and its full width at half maximum (FWHM) are demonstrated for different parametric wavelengths (the length of PPMgLN is assumed to be 15 mm), as shown in Figs.2 and 3. The parametric signal wavelengths vary from 1.4 to 4.4 μm . Fig.2 shows that the parametric gain coefficient decreases gradually with the increase of parametric wavelength. Fig.3 shows that the FWHM of parametric spectral gain strongly depends on the wavelength of the parametric signal. This FWHM increases with the parametric wavelength and reaches the maximum of about 112.5 THz near the degeneration point. However, it is quite different when the parametric wavelength deviates far from the degeneration point, where the FWHM is only several THz. For example, the FWHMs of the parametric spectral gain are about 0.96 and 1.07 THz when the wavelengths are 1.4 and 4.4 μm respectively.

These FWHMs change to about 13.68 and 10.86 THz when the parametric wavelengths are 1.9 and 2.5 μm respectively. The gain curve with two peaks is obtained at the degeneration point as shown in Fig.3 and this is believed to be the result of gain curve combination of signal wave and idle wave.

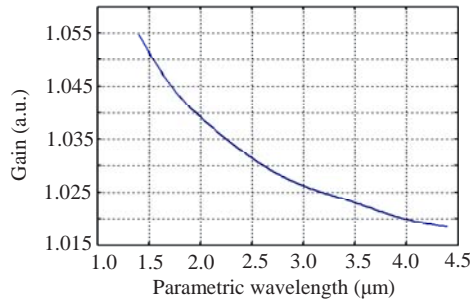


Fig.2 Variation of parametric spectral gain with parametric wavelength

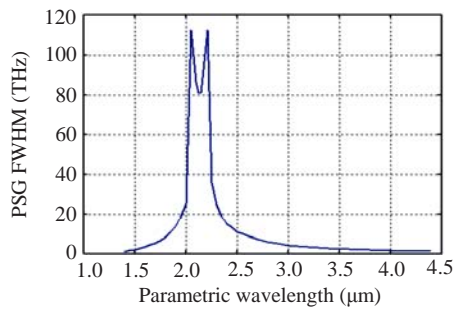


Fig.3 Variation of parametric spectral gain (PSG) FWHM with parametric wavelength

The simulation also shows that the parametric spectral gain curves change with the number of reversed domains. As demonstrated in Fig.4, when the number N changes from 1000 to 4000 at the period of 30 μm , the FWHM of the parametric spectral gain changes from 2.43 to 0.65 THz, and the output electric field intensity changes from 1.05×10^{-12} to 1.21×10^{-12} V/pm.

From the phase matching condition, it is clear that when the pump wavelength shifts, the parametric wavelength also shifts. In Fig.5, the parametric spectral gain curves under different pumping wavelengths are shown. Note that at a specific output wavelength, the shift of the pump wavelength has little effect on the parametric spectral gain bandwidth and its central wavelength. And thus, the parametric output will have a narrowest spectral output at this specific point and it is especially important when the pumping laser

source is a broadband one, just like in the situation of a fiber laser. Because the corresponding parametric wavelength separates gradually as the output wavelength deviates from the specific wavelength, such separations of the parametric wavelength will not only affect the gain coefficient but also broaden the output spectrum. It is thus very important to select an appropriate output parametric wavelength for achieving the best parameter spectral gain. In Fig.5c, one such example is shown, in which the optimal parametric spectral gain is achieved at the parametric wavelength of 1.5775 μm with a period of 30.6 μm when the pump wavelength is around 1.064 μm .

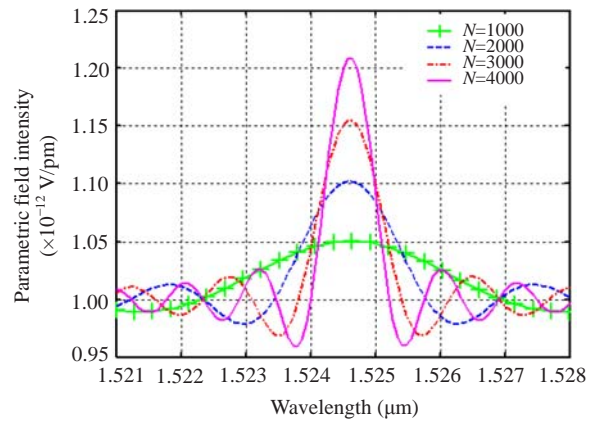


Fig.4 Dependence of the parametric spectral gain curves on the domain period numbers with a period of 30 μm

RESULTS AND DISCUSSION

The simulation results presented above would be helpful for an accurate understanding of the output characteristics of a QPM parametric system. And thus such results were partly cross-referenced to the OPO experiments carried out in home laboratory as reported in (Wu *et al.*, 2007) and were found to have good consistency. In the experiment, the spectra of two parametric laser output signals from an OPO experiment were demonstrated with one at wavelength of 1.426 μm and the other at 1.690 μm , corresponding to domain periods of 28.0 and 31.0 μm , respectively. Their FWHMs are 0.28 and 0.99 THz respectively, quite different from each other at these two wavelengths. It was also found that the parametric gain coefficient obtained using simulation as shown in this study is in good consistency with the conversion efficiency of the OPO in the experiment.

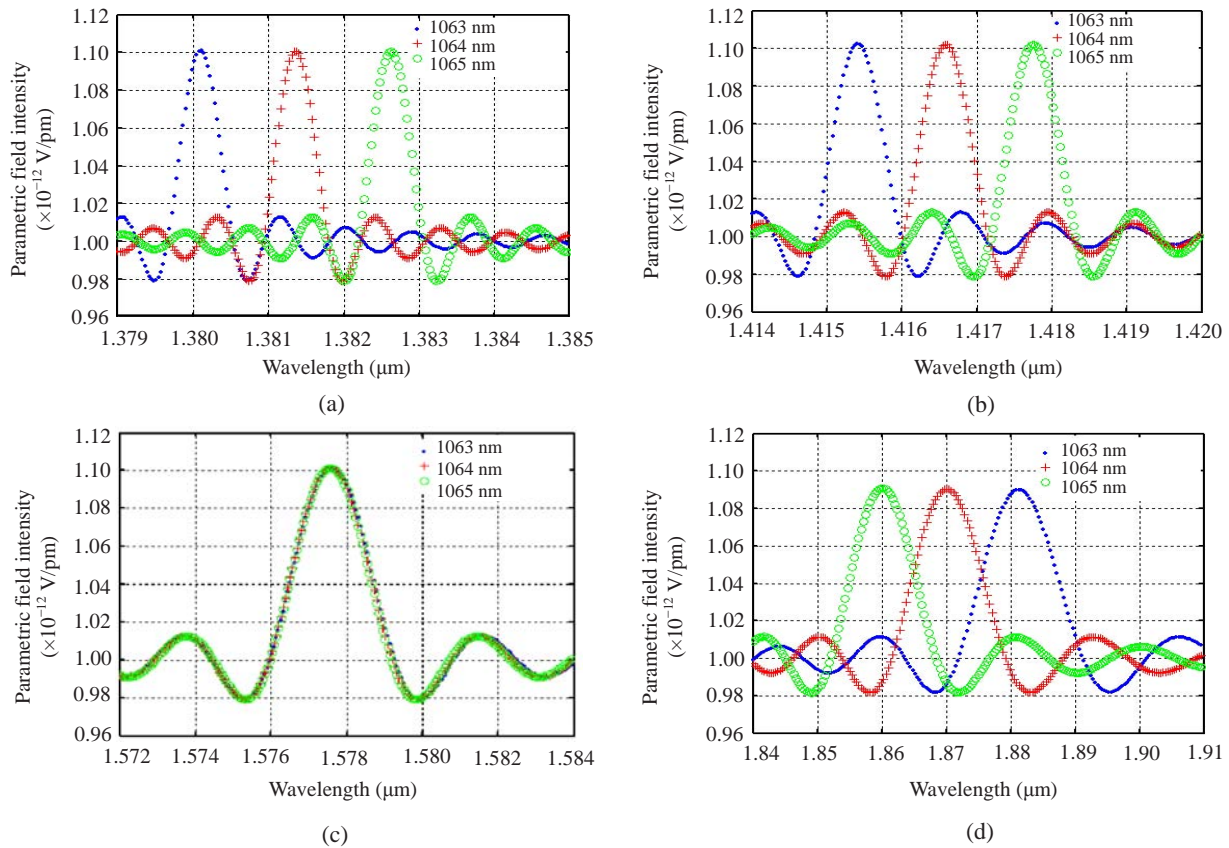


Fig.5 Parametric spectral gain curves at the pump wavelength of 1063, 1064, and 1065 nm for different periods A
 (a) $A=27.0 \mu\text{m}$; (b) $A=28.0 \mu\text{m}$; (c) $A=30.6 \mu\text{m}$; (d) $A=32.0 \mu\text{m}$

Due to the limitation of the pumping source with a large spectral width in our laboratory, the issue of optimal output wavelength has not been tested but shall be investigated upon the availability of a high power Q-switched fiber laser, which is normally broadband (up to several nm for a Q-switched fiber laser).

CONCLUSION

Through the analysis of the small-signal approximated three-wave nonlinear coupled equations on a QPM-based parametric conversion process, some interesting conclusions concerning the parametric conversion have been drawn. First, the spectral gain bandwidth of the parametric process becomes wider with the increase of parametric wavelength and reaches the maximum at the degeneration point. Second, the gain coefficient decreases gradually with

the increase of parametric wavelength. Third, the FWHM of the spectral gain decreases correspondingly with the increase of the nonlinear material length. Fourth, there exists an optimal parametric wavelength band, which is most suitable for the high gain parametric conversion when pumped by a laser source with a wide wavelength band, such as the high power fiber laser. This suggests the possible optimum configuration of an OPO for its parameters including the pump wavelength, the signal wavelength, and the domain period of the PPMgLN.

References

Armstrong, J.A., Bloembergen, N., Ducuing, J., Pershan, P.S., 1962. Interactions between light waves in a nonlinear dielectric. *Phys. Rev.*, **127**(6):1918-1939. [doi:10.1103/PhysRev.127.1918]
 Bryan, D.A., Gerson, R., Tomaschke, H.E., 1984. Increased optical damage resistance in lithium niobate. *Appl. Phys. Lett.*, **44**(9):847-849. [doi:10.1063/1.94946]
 Chen, W., Mouret, G., Boucher, D., Tittel, F.K., 2001. Mid-infrared trace gas detection using continuous-wave

- difference frequency generation in periodically poled RbTiOAsO₄. *Appl. Phys. B: Lasers Opt.*, **72**:873-876. [doi:10.1007/s003400100561]
- Feng, J., Yao, J.Q., Zheng, F.H., Li, E.B., Zhang, T.L., Zhao, P., Wang, P., Zhang, B.G., 2007. High-repetition-rate dual-signal intracavity optical parametric generator based on periodically-phase-reversal PPMgLN. *J. Opt. A: Pure Appl. Opt.*, **9**(10):797-801. [doi:10.1088/1464-4258/9/10/004]
- Huang, L., Hui, D., Bamford, D.J., Field, S.J., Mnushkina, I., Myers, L.E., Kayser, J.V., 2001. Periodic poling of magnesium-oxide-doped stoichiometric lithium niobate grown by the top-seeded solution method. *Appl. Phys. B: Lasers Opt.*, **72**:301-306. [doi:10.1007/s003400100493]
- Ishizuki, H., Shoji, I., Taira, T., 2003a. Periodical poling characteristics of congruent MgO:LiNbO₃ crystals at elevated temperature. *Appl. Phys. Lett.*, **82**(23):4062-4064. [doi:10.1063/1.1582371]
- Ishizuki, H., Taira, T., Kurimura, S., Hoonro, J., Cha, M., 2003b. Periodic poling in 3-mm-thick MgO:LiNbO₃ crystals. *Jpn. J. Appl. Phys.*, **42**(part 2):L108-L110. [doi:10.1143/JJAP.42.L108]
- Jiang, J., Hasama, T., 2003. Synchronously pumped femto-second optical parametric oscillator based on an improved pumping concept. *Opt. Commun.*, **220**(1-3):193-202. [doi:10.1016/S0030-4018(03)01342-7]
- Kulp, T.J., Bisson, S.E., Bambha, P., Reichardt, T.A., Goers, U.B., Aniolek, K.W., Kliner, D.A.V., Richman, B.A., Armstrong, K.M., Sommers, R., et al., 2002. The application of quasi-phase-matched parametric light sources to practical infrared chemical sensing systems. *Appl. Phys. B: Lasers Opt.*, **75**(2-3):317-327. [doi:10.1007/s00340-002-0978-5]
- Kuroda, A., Kurimura, S., Uesu, Y., 1996. Domain inversion in ferroelectric MgO:LiNbO₃ by applying electric fields. *Appl. Phys. Lett.*, **69**(11):1565-1567. [doi:10.1063/1.117031]
- McMullen, J.D., 1975. Optical parametric interactions in isotropic materials using a phase-corrected stack of nonlinear dielectric plates. *J. Appl. Phys.*, **46**(7):3076-3081. [doi:10.1063/1.322001]
- Milton, M.J.T., 1992. General expressions for the efficiency of phase-matched and nonphase-matched second-order nonlinear interactions between plane waves. *IEEE J. Quant. Electron.*, **28**(3):739-749. [doi:10.1109/3.124999]
- Popp, A., Müller, F., Kühnemann, F., Schiller, S., von Basum, G., Dahnke, H., Hering, P., Mürtz, M., 2002. Ultra-sensitive mid-infrared cavity leak-out spectroscopy using a cw optical parametric oscillator. *Appl. Phys. B: Lasers Opt.*, **75**(6-7):751-754. [doi:10.1007/s00340-002-1047-9]
- Stothard, D.J.M., Dunn, M.H., Rae, C.F., 2004. Hyperspectral imaging of gases with a continuous-wave pump-enhanced optical parametric oscillator. *Opt. Expr.*, **12**(5):947-955. [doi:10.1364/OPEX.12.000947]
- Wu, B., Shen, Y.H., Cai, S.S., 2007. Widely tunable high power OPO based on a periodically poled MgO doped lithium niobate crystal. *Opt. Laser Technol.*, **39**(6):1115-1119. [doi:10.1016/j.optlastec.2006.09.012]
- Xie, X.P., Fejer, M.M., 2007. Cascaded optical parametric generation in reverse-proton-exchange lithium niobate waveguides. *J. Opt. Soc. Am. B*, **24**(3):585-591. [doi:10.1364/JOSAB.24.000585]
- Zhu, Y.M., Chen, X.F., Shi, J.H., Chen, Y.P., Xia, Y.X., Chen, Y.L., 2003. Wide-range tunable wavelength filter in periodically poled lithium niobate. *Opt. Commun.*, **228**(1-3):139-143. [doi:10.1016/j.optcom.2003.09.081]